Proceedings World Geothermal Congress 2020+1
Reykjavik, Iceland, April - October 2021

# Thermo-Hydro-Mechanical Models of the Natural Circulation at Soultz-sous-Forêts and Rittershoffen EGS Sites (France)

Bérénice Vallier[1], Vincent Magnenet[2], Jean Schmittbuhl[1] and Christophe Fond[2]

[1] EOST, Université de Strasbourg/CNRS, 5 rue René Descartes, F-67000 Strasbourg, France

[2] ICUBE, Université de Strasbourg/CNRS, 72 route du Rhin, F-67411 Illkirch, France

vallier@unistra.fr

**Keywords:** thermo-hydro-mechanical model, deep geothermal reservoir, natural hydrothermal convection.

**ABSTRACT**

Numerical models of the deep geothermal reservoirs in the Upper Rhine Graben (URG) have been developed over the last few decades. However, there is still a need for models that can integrate most thermal, mechanical and large-scale geophysical data. We are developing here two-dimensional EGS reservoir models using a finite element approach that includes extended thermo-hydro-mechanical coupling (THM) including the properties of the brine as a function of the temperature and pressure of the fluid. The specificity of the approach is to assume a representative elementary volume of 100 m that homogenises the complexity of the small-scale fault network. An inversion to obtain large-scale rock properties has been performed using deep temperature logs and regional stress analyses. This modelling approach is applied to the cases of the historical Soultz-sous-Forêts (France) geothermal site and the recent nearby Rittershoffen site. Our study brings new insights on the extension of hydrothermal convection cells through the depth and on the interpretation of the temperature gradient at shallow depth. It supports a weak influence of the lithological transition between the sediments and granitic basement on hydrothermal circulation, unlike previous studies. We also show the significant effect of brine viscosity on hydrothermal circulation. Lateral temperature variability at depth in the URG is shown to be in accordance with the forecasts of this simple model. In Rittershoffen, the bottom of the hydraulic cap rock is shallower than the discontinuity of the thermal gradient such as in the Soultz-sous-Forêts case. The comparison between the two geothermal models shows many similarities in terms of rocks properties, decoupling of hydraulic and thermal cap rocks and spatial temperature variability and a weak influence of the regional fault on the hydrothermal circulation. In both cases, the inverted properties of large-scale rocks correspond to laboratory measurements. Predictions of gravity measurements of the modelled hydro-thermal circulation are proposed.

## 1. INTRODUCTION

URG is one of the most studied regions in Europe for deep geothermal applications (Huenges and Ledru, 2011; Lu, 2017). Geothermal projects, such as the well-known pilot research Soultz-sous-Forêts site, are based on an enhanced geothermal system (EGS) technology. The EGS concept consists in increasing the naturally fractured reservoir permeability using hydraulic, thermal and/or chemical stimulations in order to enhance the circulation of the natural brine significantly (Tester et al. 2006; Schindler et al. 2010; Gérard et al. 2006). The multiple research projects at Soultz-sous-Forêts site have brought an incredibly huge collection of data sets for deep EGS geothermal reservoirs (Bresee, 1992; Genter et al., 2010; Sausse et al., 2010; Schaming et al., 2016). Recently, an important database of these geophysical, geochemical and geological measurements is now available at CDGP (https://cdgp.u-strasbg.fr/) or from EPOS TCS-AH platform (https://tcs.ah-epos.eu/). It allows, in particular, to calibrate reservoir models and subsequently understand the THM behaviour of the present and future EGS reservoirs. After the development (during more 25 years) of the Soultz-sous-Forêts pilot site as an EGS demonstrator, a new industrial project at Rittershoffen, located 6 km east from Soultz-sous-Forêts, was initiated in 2011 and operated in 2016 (Baujard et al. 2015; Genter et al. 2015). Structural and stratigraphic studies (Aichholzer et al. 2016; Vidal et al. 2016), temperature logs (Baujard et al. 2016, 2017) as well as seismic (Gaucher et al. 2013; Maurer et al. 2015; Lengliné et al. 2017) and geochemical surveys (Dezayes et al. 2014; Sanjuan 2016) have been already conducted. The knowledge of the Rittershoffen site is also completed by the database collected at Soultz-sous-Forêts.

For EGS projects, numerical models provide a useful tool for integrating data, studying the natural hydro-thermal circulation, testing new concepts and managing short- and long-term developments of the reservoir (Pruess, 1990; Kolditz and Clauser, 1998; Sanyal et al., 2000; Jain et al., 2015; Tomac and Sauter, 2017). Most of the models are categorized into three main classes according to their geological fracture network description using (Willis-Richards and Wallroth, 1995): (i) stochastic distributions (Baujard and Bruel, 2006; Cacas et al., 1990), (ii) regular grids (Watanabe and Takahashi, 1995; Willis-Richards et al., 1996; Kohl and Mégel, 2007) or (iii) deterministic sets (Gentier et al., 2005). These models aim at solving the physical balance equations using more or less complex fracture network geometries. Few other models are based on a homogenised description of the medium and analyse in detail the coupled physical processes such as the very rich thermo-hydro-mechanical-chemical (THMC) couplings (Kohl et al., 1995; Gelet et al., 2012; Diersch and Kolditz, 1998; Bächler and Kohl, 2005).

The goal of the present study is to focus on one specific objective of deep geothermal models: the description of the natural hydro-thermal circulation within the two EGS Soultz-sous-Forêts and Rittershoffen reservoirs. Our motivation is based on the recent evolution of EGS reservoirs which are managed to enhance at best the reservoir productivity (Schill et al., 2017) but minimizing the transformation of the natural system in order to reduce at maximum induced risks and to extend the operation life of the geothermal plant at minimal cost (Huenges and Ledru, 2011). Such optimization requires the best knowledge of the initial natural system. Our model integrates dominant thermo-hydro-mechanical (THM) couplings in two-dimensions using a finite element approach to predict the large scale and steady-state natural hydro-thermal circulation. The specificity of our approach is twofold. First, the reservoir is homogenised at the scale of 100 metres, i.e. without considering details of inhomogeneities under this scale of

description like the local structure of the fracture networks. Secondly, special care is taken to describe in detail the rheology of the in-situ fluid (e.g. density, viscosity, heat capacity), which depends on temperature and fluid pressure as shown by laboratory measurements. We also include different settings: (i) the main geological structures from the sedimentary cover (Aichholzer et al., 2016; Vidal et al., 2015; Vidal et al. 2016) to the granitic basement (Dezayes et al., 2005b; Sausse et al., 2010) including the fractured and altered domains (Dezayes et al., 2010; Cuenot et al., 2008a) (ii) the temperature-depth profiles through the deep boreholes GPK-2, 3 and 4 for Soultz and GRT-1 and 2 (Pribnow and Schellschmidt, 2000; Schindler et al., 2010; Baujard et al. 2017) (iii) the distribution of the natural radioactivity (Rummel, 1992; Pribnow et al., 1999; Pribnow and Schellschmidt, 2000) (iv) the regional stress-state (Evans et al., 2009; Cornet et al., 2007; Valley, 2007) (v) the rock properties and their up-scaling (Haenel, 1983; Rummel, 1992; Kirk and Williamson, 2012; GeORG, 2013) (vi) the geochemical data from brine samples (Aquilina et al., 1997; André and Vuataz, 2005; Sanjuan et al., 2006). The physical balance equations are solved using the finite element Code Aster for the direct approach. We then invert reservoir parameters from temperature and stress measurements. We finally discuss: (i) the sensitivity of the complex rheology on the hydro-thermal circulation; (ii) the influence of regional fault on the hydrothermal circulation.

## 2. A THM LARGE-SCALE MODEL

### 2.1 An overview of Soultz and Rittershoffen EGS sites

#### 2.1.1 Soultz-sous-Forêts

Fig. 1a shows a representation of the main geological units at Soultz and Fig. 1b features the temperature-depth profiles measured from the GPK-1,-2,-3 and -4 wells. The first 1.4 kilometres are made up of the sediments overlying granites. Two main natural fracture systems have been recognised in the Soultz granite (Dezayes et al., 2005). The first system is a closely connected network of small-scale fractures. The second one is a set of large-scale fractures including the fault FZ4770 that intersects GPK3 well at a depth of 4770m and reaches the open hole of GPK2 at 3900m. FZ4770 is responsible for around 70% of fluid losses during hydraulic tests (Sanjuan et al., 2015).

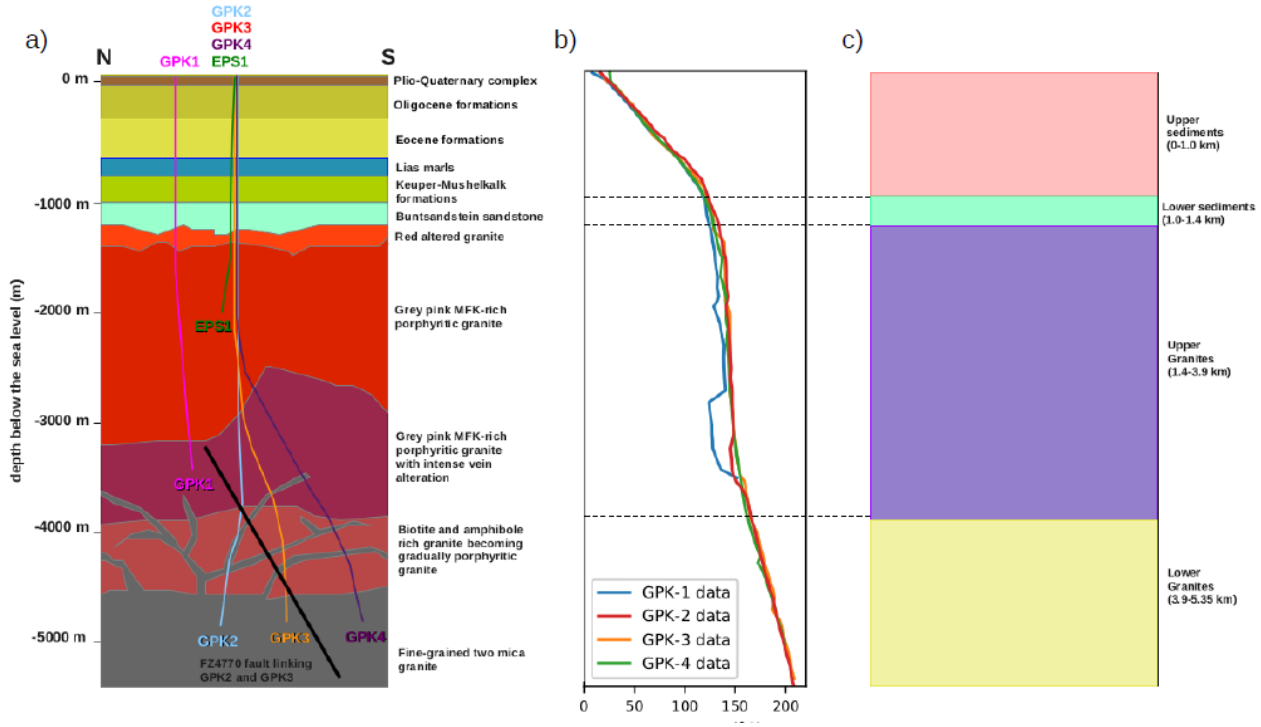


**Fig. 1: a) 2D conceptual model of the geology at Soultz-sous-Forêts site (modified after Dezayes et al. (2005a), Aichholzer et al. (2016) and Vallier et al. (2019)). Trajectories of GPK1, EPS1, GPK2, GPK3 and GPK4 wells are shown with coloured lines. The major fault through the reservoir (FZ4770) is drawn as a black line (Sausse et al., 2010). b) Equilibrium temperature profiles obtained from logs in Soultz-sous-Forêts wells (GPK2, GPK3, GPK4) after drilling operation (Cuenot et al., 2008a). c) The simplified geological model for the present work with four main geological units.**

Regarding the thermal state of the reservoir, the first striking observation is that despite the spatial separation at a depth of the wells, they globally superimpose and all exhibit three major common trends with depth. In the upper part of the sedimentary cover, the geothermal gradient is constant at around 110°C.km$^{-1}$. From the sediment–granite interface to around 3.9 km deep, the gradient declines to less than 10°C.km$^{-1}$. Some local temperature disturbances (less than 10 °C) from the general trend have been recorded around 2.0 km and 3.4 km deep (Vidal et al., 2015). They are generally considered as local thermal signatures of fault zones (Evans et al., 2005). The overall strong similarities between the T-logs suggest however that the large-scale faults have a weak influence on the temperature profiles since the thermal regime is structured at a larger scale than the fault zones. After 3.9 km deep, the geothermal gradient progressively tends to the average Central European gradient, which is of the order of 30°C.km$^{-1}$. The

radioactive production rates are respectively set at 0.1, 1.0, 5.0 $\mu Wm^{-3}$ for the upper sediments, the lower sediment unit and the two granite units (Rummel, 1992; Pribnow et al., 1999; Pribnow and Schellschmidt, 2000).

Several studies have been performed to characterise the natural stress state at Soultz (Cornet et al., 2007; Valley, 2007; Evans et al., 2009). They rely on the analysis of BoreHole TeleViewer (BHTV) images, gamma density logs, distribution and magnitude of breakouts through the different boreholes (EPS1, GPK1, GPK2, GPK3 and GPK4). The linear trends with the depth of the principal stress magnitudes from Evans et al. (2009) have been used here.

### 2.1.2 Rittershoffen

The Rittershoffen site is located at 6 km South-East from Soultz-sous-Forêts, and it is operated since 2016 (Genter et al., 2015; Baujard et al., 2017). The site is based on a doublet (GRT-1 and GRT-2) that targets the sediment-granite interface (Baujard et al. 2015) at 2.2km depth. The petrology is partially deduced thanks to cores from the close-by EPS-1 and GPK-1 wells at Soultz-sous-Forêts (Aichholzer et al. 2016). The stress field is assumed to be the same as the regional trends estimated at Soultz (Evans et al. 2009; Cornet et al. 2007). However, numerous specific geophysical, geochemical or stratigraphical studies have been conducted on the Rittershoffen site (Aichholzer et al. 2016; Vidal et al. 2016; Lengliné et al. 2017; Sanjuan et al. 2016).

Fig. 2a features the conceptual and simplified geology model of the Rittershoffen geothermal site (Vallier et al. 2018). The first 2.2 kilometres consist of the sedimentary cover (against 1.4 kilometres at Soultz) overlying the granitic basement. The shallowest granites are strongly fractured with about 2.5 fractures per meter (Vidal et al. 2016). Two main natural fracture systems have been identified, one made of closely connected meso-fractures and the other of a set of large fractures crossing the former system (Dezayes et al. 2014). After 2.5 km in depth, i.e. below the wells, the characterisation of the deep granitic basement is mostly based on the knowledge from the deep wells in the close-by Soultz site.

Fig. 2b illustrates the temperature-depth profiles from the GRT-1 and GRT-2 wells (Baujard et al. 2017). Above the top of the Muschelkalk, the geothermal gradient is mostly constant, about 85°C.km$^{-1}$, however, decreases sharply at 1.65 km in depth to 3°C.km$^{-1}$. The constant thermal gradient in the first kilometres has firstly been interpreted as an indicator of a purely diffusive heat transfer. Its sharp change at 1.65 km deep is seen as an effect of hydrothermal convection. The geochemical analysis also evidences a strong circulation between the wells (Sanjuan et al. 2016). The Rittershoffen stress state is assumed to be consistent with the regional trends (Baujard et al. 2017) and its evolution with depth has been estimated from the nearby Soultz site (Evans et al. 2009; Cornet et al. 2007).

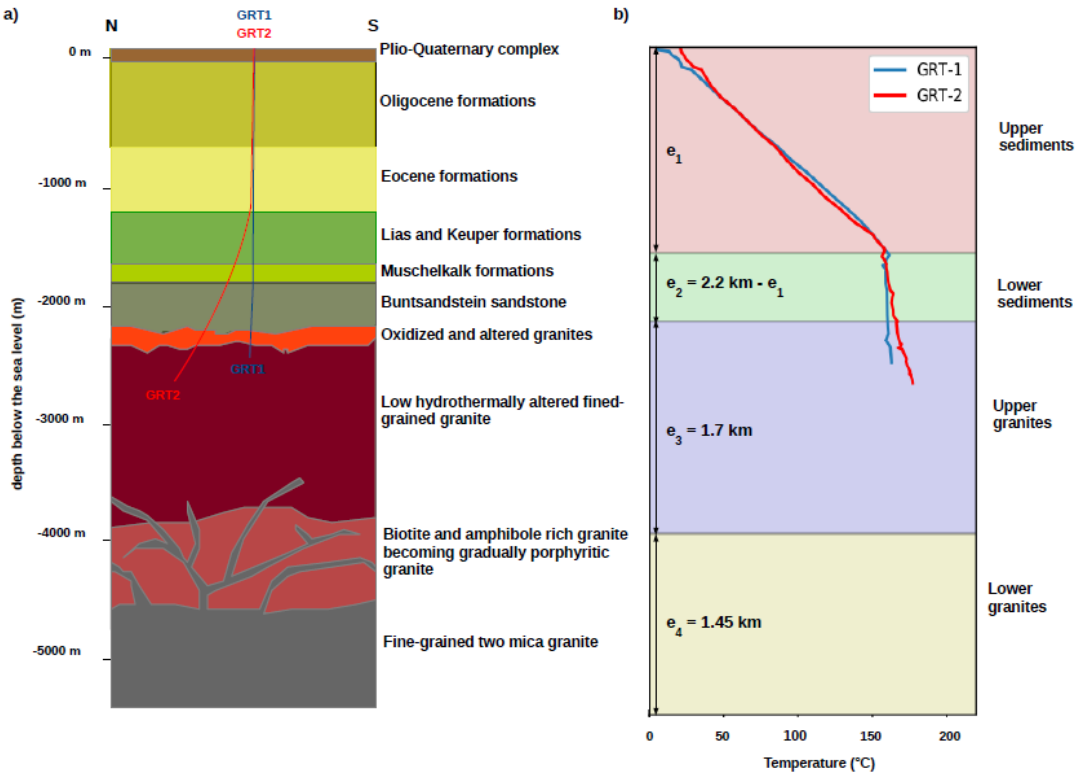


**Fig. 2: a) 2D conceptual model of the geology at Rittershoffen site (after Vallier et al. (2018)). The sedimentary cover is investigated from geological studies from Vidal et al. (2017) and Aichholzer et al. (2016). The granite below 2.5 km deep is assumed to be the same as in the Soultz-sous-Forêts site (Dezayes et al. 2005a). b) Temperature–depth profiles obtained from logs run in the Rittershoffen wells (GRT-1, GRT-2) after drilling operation over (Baujard et al. 2017). The background colours correspond to the four layers homogenized at the scale of about 100 m and considered in the model ( e1 , e2 , e3 and e4 correspond to the layer thicknesses, e1 is inverted during the back analysis; e2 = 2.2 km - e1 ; e1 + e2 + e3 = 3.9 km ; e1 + e2 + e3 + e4 = 5.4 km)**

### 2.2 Towards a homogenised reservoir model

The goal of the study is to build the simplest THM numerical models consistent with the main characteristics for the Rittershoffen and Soultz sites. The models do not aim at describing all the complexity of the geology or the deterministic details of the fault networks. As sketched in Fig. 1c and 2b, the whole sedimentary cover is reduced to two homogenized horizontal units: the upper sediments and the lower sediments. The depth of the transition between the two units is taken as a parameter to be adjusted (named e1) during the back analysis. The basement is also split into two units: the upper granites and the lower granites. Due to the lack of direct knowledge on the deep granitic basement in Rittershoffen, the transition between the two units is set at a depth e1 + e2 + e3 = 3.9 km. The transition between the sediments and the granite is also set at e1 + e2 = 2.2 and 1.4 km in depth for Rittershoffen and Soultz, respectively.

### 2.3 Coupled THM processes

The homogenised units are assumed to be a fully saturated porous medium with a single-phase brine. The model describes the coupled THM processes from a linear thermo-poro-elastic approach in the limit of the small perturbation as developed by Coussy (2004). The complete set of equations governing the THM coupling is presented in Vallier et al. (2019). Here, the Cauchy stress is split into effective stress and hydraulic stress. Homogenised properties are depending on temperature, fluid pressure and porosity thanks to classic mixing laws. One specificity of our THM model is that the brine rheology depends on temperature and fluid pressure using laboratory measurements of the rheology of a NaCl pure solution with a mass content of 100 $g.L^{-1}$ (Zaytsev and Aseyev 1992; Kestin et al. 1981; Rowe and Chou 1970). The temperature dependence of th brine rheology for the dynamic fluid viscosity has been shown to have a strong influence on the hydrothermal circulation (Vallier et al. 2019).

### 2.4 Numerical aspects

#### 2.4.1 Direct model

The simulations are carried with the open-source finite element *Code_Aster* software (EDF 2014). The equations governing the THM coupling are solved with a Euler implicit scheme, and the increment of the generalised displacements is calculated using the Newton-Raphson algorithm. Initially, constant and uniform temperature and fluid pressure distributions are respectively set at 10.0°C and 0.1 MPa. The calculation is split up in three successive steps to improve the convergence of the process (Magnenet et al., 2014): (i) during a short time period of 1000 years, the boundary conditions and gravity are progressively applied; (ii) next, during 100,000 years, the system freely evolves along constant boundary conditions; (iii) in one last increment, a steady-state solution is obtained by cancelling the time-dependent terms from the THM equations.

The typical size of the quadratic THM element is 100 meters. The boundary THM conditions are: (i) for the thermal state, the temperatures are, maintained on the upper and lower boundaries. The lateral boundaries are taken s adiabatic; (ii) for the hydraulic state, fluid pressure is set on the upper boundary; the other boundaries are assumed to be impermeable; (iii) for the mechanical part, the normal displacement is fixed to zero on the lower and lateral boundaries. The upper boundary is stress-free.

#### 2.4.2 Back-analysis

To characterise the hydrothermal circulation and the mechanical state of the reservoir, we aim at reproducing the observed thermal and stress data and estimate the rock physical and geometrical parameters at the reservoir scale. We proceeded to a back-analysis using the open-source PEST software (Doherty 2005). The approach is based on the Levenberg-Marquardt algorithm minimising the error function, i.e. the L2-norm of the discrepancy between simulated and observed temperature and stress-depth profiles according to a prior set of parameters. The four rock properties explored during the back-analysis are the permeability, thermal conductivity, Young's modulus and Poisson's ratio to reproduce the temperature and stress – depth profiles observed in Rittershoffen and Soultz. The depth of the transition between the two sedimentary units is also adjusted during the back-analysis. The other rock properties and depths of interfaces are set as constant during the back-analysis. Low CPU time consuming, this method is however sensitive to its initial conditions, i.e. the prior distributions. The knowledge from Soultz allows constraining the prior distributions for the rock properties.

## 3. RESULTS FROM THE BACK-ANALYSIS

### 3.1 Soultz-sous-Forêts

Fig. 3a shows the very good fit of the observed temperature-depth profile at GPK2 that is obtained. The predicted maps of temperatures and Darcy velocities are plotted in Fig. 3b. They illustrate that the simulated hydrothermal convection is involving not only the upper granite but also most of the sediments. The convection cells have a width of 3.0 km and a height of 3.8 km. The maximum of Darcy's velocity is 11.0 $cm.yr^{-1}$, a value close to estimations from previous modelling and hydraulic tests (Clauser 1990; Guillou-Frottier et al. 2013; Baria et al. 1998). The inverted depth of the transition between the upper and lower sediments is now at 100m. This corresponds to the hydraulic cap rock leading to a significant convective flow much closer to the surface than previously expected in the studies of Soultz. Simultaneously the observed trends of the principal stress components with depth (Evans et al. 2009; Cornet et al. 2007) are reproduced by a back-analysis of the elastic moduli (Young modulus and Poisson ratio). The model is also assumed to be oriented along the direction of the maximum horizontal principal stress. Fig. 4 shows the best fit of the in-situ stress-depth profiles for the three principal components.

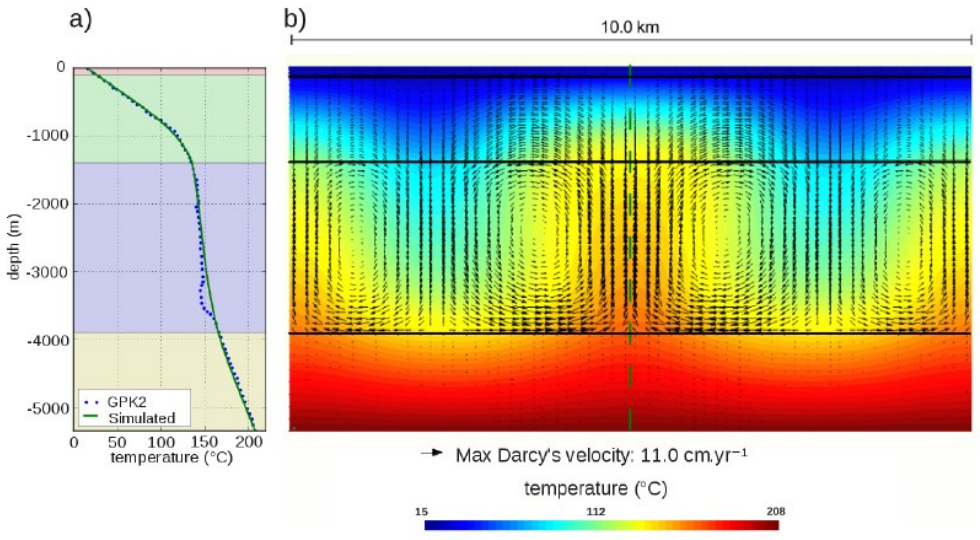


**Fig. 3: a) Comparison between the observed T-log in GPK-2, Soultz-sous-Forêts, (dotted blue line) and the best fitting simulated vertical temperature-depth profile (green line). The purple dashed lines correspond to the lithological limits. b) Associated temperature and Darcy's velocity (black arrows) maps. The vertical dashed green and horizontal black lines are respectively the positions of the profile and the depth limits of the units.**

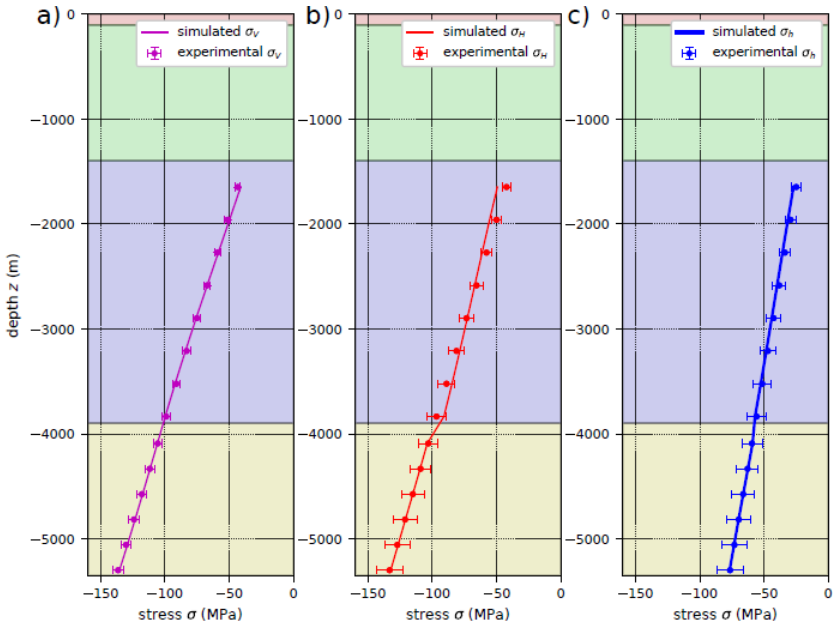


**Fig. 4: Evolution of principal stress components with depth: (a) vertical and (b) horizontal minimum and (c) maximum stress profiles located at the middle of the Soultz model.**

### 3.2 Rittershoffen

Fig. 5a shows the excellent fit of the GRT-1 T-log after back-analysis, adjusting the rock-properties and the depth of the transition between the upper and lower sediment units. Without any large-scale fault, the homogenised THM model reproduces the observed profiles. Fig. 5b illustrates the temperature and Darcy's velocity maps associated with the best fit of the observed data. A large-scale convective system is obtained with convection cells having a width and height respectively of 3.0 km and 2.7 km. The maximum of Darcy's velocity of the natural convection is 20.0 cm.yr$^{-1}$. The obtained thickness of the hydraulic cap-rock is 1.2 km; its bottom does not correspond to the breaking point of the T-log as previously expected (Baujard et al., 2017). The stress-depth trends are taken from the measurements at the Soultz site. They are assumed to be similar for the Rittershoffen site (Baujard et al., 2017). Fig 6 shows the best fit for each of the three stress components.

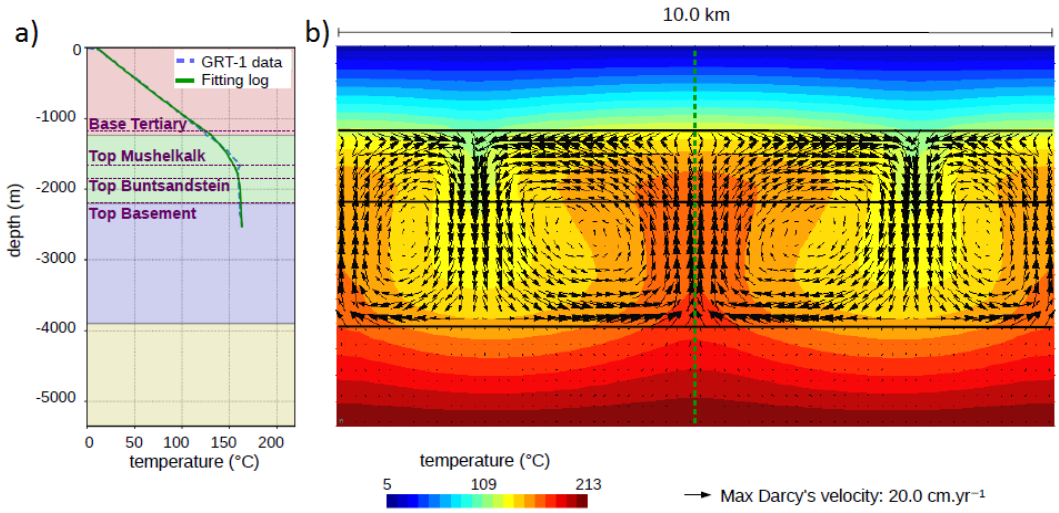


**Fig. 5: a) Comparison between the observed T-log in GRT-1, Rittershoffen, (dashed blue line) and the best fitting simulated vertical temperature-depth profile (green line). The purple dashed lines correspond to the lithological limits. b) Associated temperature and Darcy's velocity (black arrows) maps. The dashed green and black lines are respectively the position of the profile and the limits of the units.**

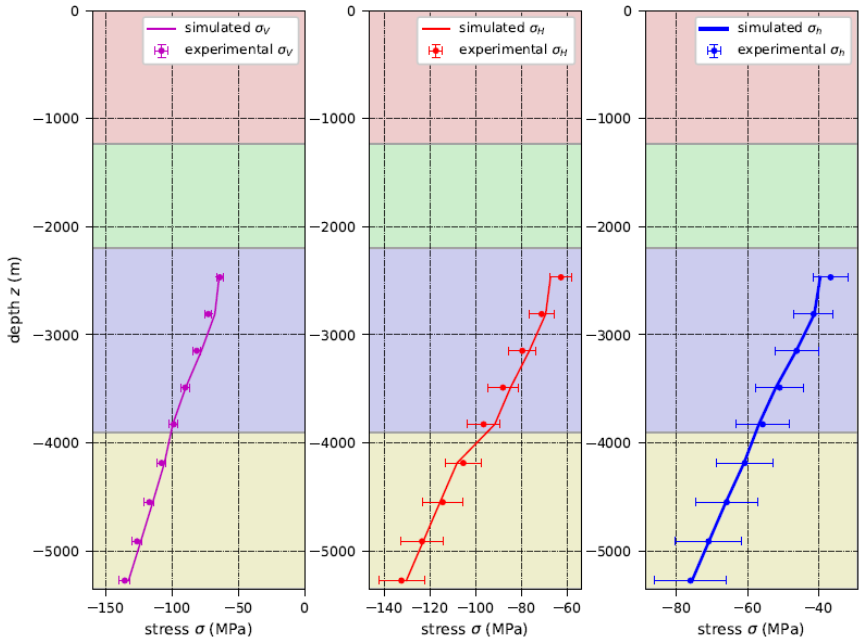


**Fig. 6: Evolution of the principal stress components with depth: (a) vertical and (b) horizontal minimum and (c) maximum stress profiles located at the middle of the Rittershoffen model.**

### 3.3 Comparison of rock properties between the two sites

Fig. 7 illustrates the estimated permeability and thermal conductivity–depth profiles for both Rittershoffen and Soultz sites. At Soultz site, the inverted permeabilities are, respectively, $1.0 \times 10^{-17}$ m$^2$, $3.5 \times 10^{-15}$ m$^2$, $6.0 \times 10^{-15}$ m$^2$ and $2.5 \times 10^{-16}$ m$^2$ for the upper sediments, the lower sediments (below 100 m deep), the upper and the lower granites. The permeability increases with depth from the upper sediments to the lower sediments and upper granites. Importantly, the permeability of the lower sediments and the upper granite are very similar, suggesting that the lithological transition between the sedimentary cover and the granitic basement is not significant for the hydraulic properties. The permeability decreases after 3.9 km in depth at the root of the geothermal reservoir. For the thermal conductivity at Soultz site, the values are 3.1 W.m$^{-1}$ K$^{-1}$ for the granites and 2.1 W.m$^{-1}$ K$^{-1}$ for the sediments. The thermal conductivity increases significantly at the interface between the sediments and granitic basement. Below, its value remains constant in both granitic units. The thermal property shows a contrast at the interface between the sediments and granites on the contrary to permeability. Profiles for the two properties highlight that both geothermal sites share noticeable similarities. Both sites show a blanketing effect from the whole sedimentary cover, whereas the top of the convective cells (i.e., the bottom of the hydraulic cap rock) is at the transition between the upper and lower sediments. The other similarity between both geothermal sites concerns the rock properties. The reservoir permeability is similar between both sites, about $1.0 \times 10^{-14}$ m$^2$ in the granitic basement and the lower sediments. The permeability is also very close in the deep granites, about $6.0 \times 10^{-15}$ m$^2$. The more important fracture

density can explain the slightly higher permeability for the Rittershoffen reservoir in the granite compared to Soultz (Vidal et al. 2016). There is a noticeable discrepancy between the two sites: the thicknesses of the hydraulic cap rocks. The difference is more than 1 km and leads to a discrepancy between the permeabilities in the upper sediments. This difference can be explained by a higher fracture density for the sediments in Soultz than in Rittershoffen. This is consistent with the recent stratigraphic studies comparing the two geothermal sites (Aichholzer et al. 2016). Indeed, a more intense fault network has been observed for the sediments in Soultz (Aichholzer et al. 2016; Vidal et al. 2016). Fig. 8 also provides a comparison of the estimated moduli for Rittershoffen and Soultz sites. The Young's modulus and Poisson's ratio are very similar for the granitic basement between sites.

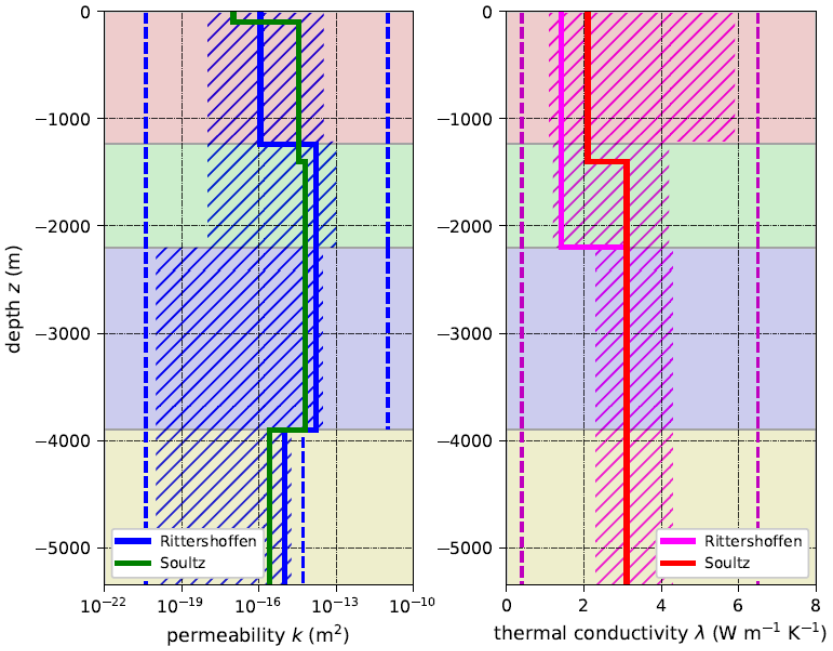


**Fig. 7: Comparison of permeability estimated by back analysis (left) and thermal conductivity (right) between Rittershoffen and Soultz. The shadow zones correspond to the range of experimental values (permeability in green, and thermal conductivity in red). The dashed lines correspond to the prior distributions for the back analysis. Background colours correspond to geological units.**

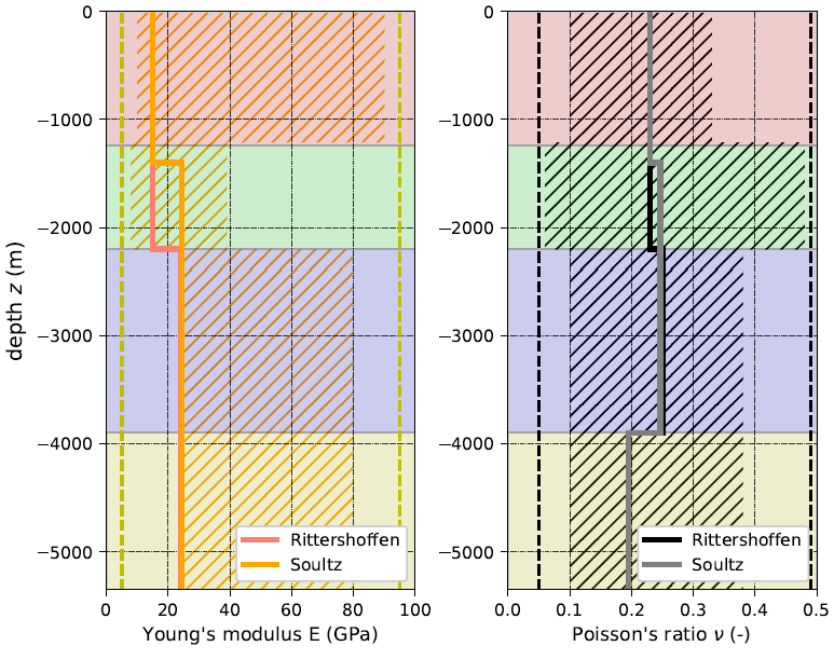


**Fig. 8: Comparison of Young's modulus (left) and Poisson's ratio (right) between Rittershoffen and Soultz. The shadow zones correspond to the range of experimental values (Young modulus in yellow, and Poisson ratio in grey). The dashed lines correspond to boundaries of the prior distributions for the back analysis.**

## 4. DISCUSSION

### 4.1 Influence of the brine viscosity

Few studies address the role of the brine viscosity on the hydrothermal circulation, and more specifically its nonlinear behaviour, i.e. the nonlinear sensitivity of the viscosity to temperature and pressure (Jaupart and Mareschal, 2010). In the present work, the dynamic fluid viscosity is nonlinear with an exponential decrease with temperature. To illustrate the influence of the fluid viscosity on the hydro-thermal circulation, we compare the best model obtained for Soultz site with two test cases (see Fig. 9). In the first test case, the viscosity is set constant with the value from the nonlinear law at the surface temperature. In the second case, the viscosity is also set constant but at the value for the temperature at the bottom of the reservoir (see Fig. 9a). Fig. 9b features the temperature-depth profiles for each case and compares them to the observed temperature-depth profile at GPK2. Fig. 9c shows the computed temperature maps for each case and their Darcy's velocity fields. Three distinctive families of thermal solutions are obtained. Assuming a constant high viscosity of shallow depth for the brine leads to a purely diffusive thermal state. Indeed, increasing the fluid viscosity reduces the Rayleigh number and translates the system through the critical Rayleigh boundary leading to purely conductive heat transport in the reservoir. In the case of low viscosity (i.e. viscosity of the brine at the bottom of the reservoir), a convective solution is obtained similarly to the previous solution. However, the temperature profile corresponds to "cold" convection, where the cold surface boundary influences the reservoir deeply. Indeed, the mean temperature in the reservoir is in this case about 110°C, i.e. almost 35°C less than the solution with temperature-dependent viscosity. The latter appears as "warm" convection responsible for a larger positive thermal anomaly, consistently with the observed temperature profile at GPK2.

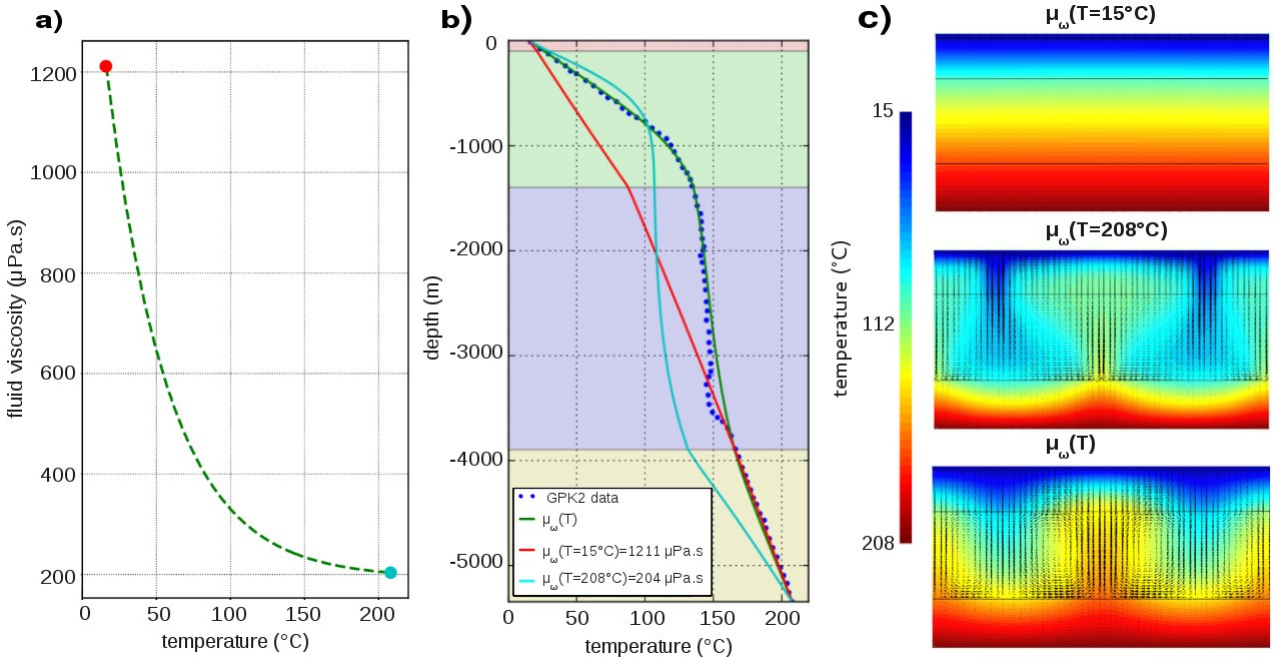


**Fig. 9: a) Fluid viscosity vs temperature for the three studied cases: in red, a constant viscosity at shallow depth temperature; in blue, a constant viscosity at large depth temperature, in green, nonlinear viscosity with an exponential dependence on temperature; b) comparison of temperature-depth profiles from THM models with observed temperature profile at GPK2 changing the viscosity laws. (c) Associated maps of temperatures (background colours) and Darcy's velocities (arrows).**

### 4.1 Influence of a large-scale fault

Fig. 10 features the temperature and Darcy's velocity maps when the Rittershoffen fault is included and described with a dip of 45°. An ascending hydrothermal circulation is shown to exist along the fault. The associated maximum of Darcy's velocity is estimated to be of the order of 26.0 cm.yr$^{-1}$, slightly higher than in the case without fault. Importantly the perturbation is local. The reservoir-scale convective system shows the same number of convective cells with similar dimensions to the model without any large-scale fault. Fig. 11 illustrates the simulated temperature-depth profile when the Rittershoffen fault is described for the three different dips. The discrepancy between the different dips is less than 2°C. After adding a fault, the temperature shift is at a maximum of about 6°C at 2.0 km in depth. The temperatures are slightly higher in the sedimentary cover and weaker in the basement, but the general profile trend stays mostly undisturbed.

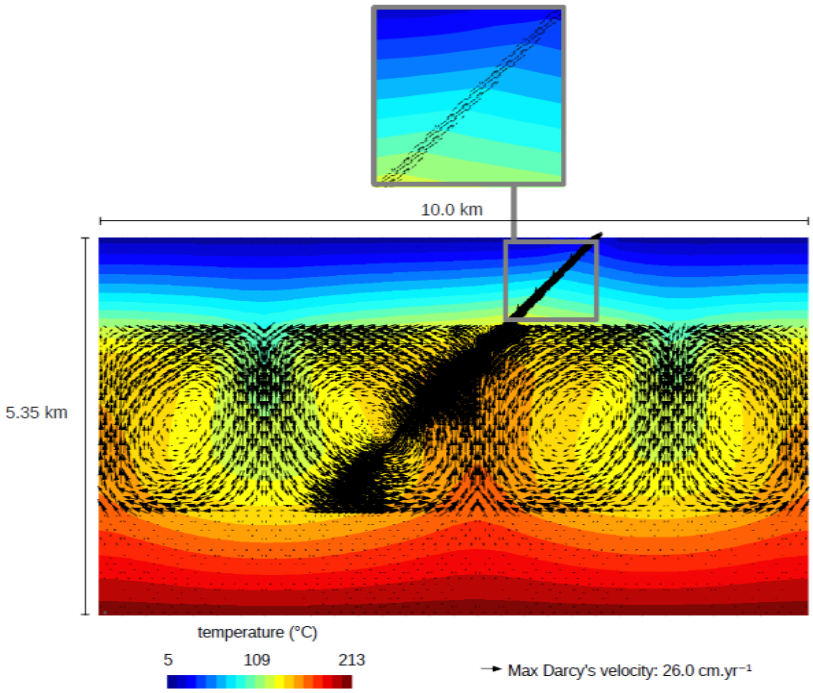


**Fig. 10: Simulated temperature and Darcy's velocity maps for the model describing the Rittershoffen fault with a dip of 45°. A closer zoom has been made near the fault in the sediments (after Vallier et al., 2018).**

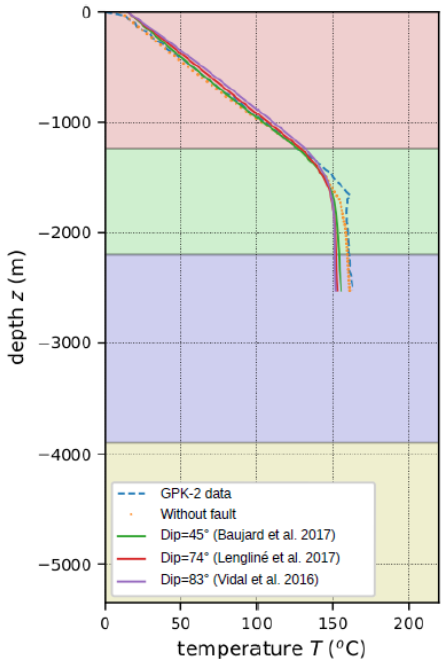


**Fig. 12: Comparison between the simulated temperature-depth profiles from models including the Rittershoffen fault with different dips and the model without the fault. All the profiles are extracted at the location of the maximum of the ascending flow.**

## 5. CONCLUSION

By using a back analysis confronting a THM model to the temperature and stress profiles observed at Rittershoffen and Soultz, an excellent fit of the T-log has been found as well for the stress–depth trends. The bottoms of the hydraulic cap rock (i.e., the top of the convection cells where a contrast of permeability is obtained) are identified shallower than the interface sediments-granite as previously proposed for both sites. Contrary to the hydraulic cap rock, the bottom of the thermal cap rock (i.e., the zone of thermal conductivity contrast) occurs at the interface between the sediments and the granite. The permeability, thermal conductivity and elastic moduli have the same general trend with depth and similar values at Soultz and Rittershoffen. Both sites highlight the same

decoupling of the hydraulic and thermal cap rocks. The model also emphasises the significant influence of the variation of brine viscosity with temperature. Indeed, the nonlinear viscosity of the brine is shown to be responsible for the significant thermal anomaly with a strong pseudo-constant geothermal gradient deep in the sediments together with a significant convective flow. The study also allows us to validate that the regional faults are not significantly controlling the hydrothermal circulation which supports the homogenization approach of our THM model.

## ACKNOWLEDGEMENTS

The present work has been done under the framework of the LABEX ANR-11-LABX-0050-G-EAU-THERMIE-PROFONDE and benefits from a state funding managed by the French National Research Agency (ANR) as part of the “Investments for the Future” program. The EGS Alsace Grant from ADEME has also funded it. The authors would like to thank Christoph Clauser, Albert Genter, Clément Baujard, Thomas Kohl, Chrystel Dezayes, David Bruhn, Nima Gholizadeh Doonechaly, Bernard Sanjuan, Benoit Valley, Judith Sausse, Philippe Jousset, Dominique Bruel, Eva Schill, Patrick Baud, Mike Heap, Luke Griffiths, Alexandra Kushnir, Olivier Lenglinè, Coralie Aichholzer, Philippe Duringer and François Cornet for very fruitful discussions.

## REFERENCES

Aichholzer C, Duringer P, Orciani S, Genter A. New stratigraphic interpretation of the Soultz-sous-Forêts 30-year-old geothermal wells calibrated on the recent one from Rittershoffen (Upper Rhine Graben, France). Geothermal Energy. 2016 ;4(1):13.

André, L., Vuataz, F.. Simulated evolution of reservoir properties for the Enhanced Geothermal System at Soultz-sous-Forêts: the role of hot brine-rock interactions. In: Thirtieth Workshop on Geothermal Reservoir Engineering Stanford University. 2005. p. 283–290.

Aquilina, L., Pauwels, H., Genter, A., Fouillac, C.. Water-rock interaction processes in the Triassic sandstone and the granitic basement of the Rhine Graben: Geochemical investigation of a geothermal reservoir. Geochimica et Cosmochimica Acta 1997;61(20):4281–4295.

Baria R, Baumgärtner J, Gérard A, Jung R. The European HDR programme 1992-1995. Technical Report; Joule III Programme, final report EUR 18925 EN; 1998.

Baujard C, Bruel D. Numerical study of the impact of fluid density on the pressure distribution and stimulated volume in the Soultz HDR reservoir. Geothermics. 2006;35(5):607–21.

Baujard C, Genter A, Graff J.J, Maurer V, Dalmais E. ECOGI a new deep EGS project in Alsace, Rhine Graben, France In: Proceedings world geothermal congress. 2015.

Baujard C, Genter A, Dalmais E, Maurer V, Hehn R, Rosillette R. Temperature and hydraulic properties of the Rittershoffen EGS reservoir, France In: European geothermal congress. 2016.

Baujard C, Genter A, Dalmais E, Maurer V, Hehn R, Rosillette R, Vidal J, Schmittbuhl J. Hydrothermal characterization of wells GRT-1 and GRT-2 in Rittershoffen, France: implications on the understanding of natural flow systems in the Rhine Graben. Geothermics. 2017; 65:255–68.

Bresee, J.C.. Geothermal Energy in Europe: The Soultz Hot Dry Rock Project. CRC Press, 1992.

Cacas M, Ledoux E, de Marsily G, Tillie B, Barbreau A, Durand E, Feuga B, Peaudecerf P. Modeling fracture flow with a stochastic discrete fracture network: Calibration 1. The flow and validation model. Water Resour Res. 1990; 27:479–89.

Clauser C, Villinger H. Analysis of conductive and convective heat transfer in a sedimentary basin, demonstrated for the Rheingraben. Geophys J Int. 1990;100(3):393–414.

Cornet FH, Bèrard T, Bourouis S. How close to failure is a granite rock mass at a 5 km depth? Int J Rock Mech Mining Sci. 2007;44(1):47–66.

Coussy O. Poromechanics. Chihester: Wiley; 2004.

Cuenot N, Charléty J, Dorbath L, Haessler H. Faulting mechanisms and stress regime at the European HDR site of Soultz-sous-Forêts, France, Geothermics, Vol. 35, No. 5-6, 561-575. 2004.

Dezayes C, Gentier S, Genter A. Deep geothermal energy in Western Europe: the Soultz project. Orleans: Technical Report; 2005a.

Dezayes C, Sanjuan B, Gal F, Lerouge C, Fluid geochemistry monitoring and fractured zones characterization in the GRT-1 borehole (ECOGI project, Rittershoffen, Alsace, France). In: Deep Geothermal Days, Paris, France. 2014.

Diersch HJG, Kolditz O. Coupled groundwater flow and transport: 2. Thermohaline and 3d convection systems. Adv Water Resour. 1998;21(5):401–25.

Doherty J. Model independent parameter estimation. 2005. http://www.pesthomepage.org.

EDF R. Code_Aster Open Source - general FEA software. 2016. http://www.code-aster.org.

Evans K, Valley B, Häring M, Hopkirk R, Baujard C, Kohl T, Magel T, Andrè L, Portier S, Vuataz F. Studies and support for the EGS reservoirs at Soultz-sous-Forêts. Centre for Geothermal Research CREGE CHYN: Technical report; 2009.

Gaucher E, Maurer V, Wodling H, Grunberg M. Towards a dense passive seismic network over Rittershoffen geothermal field In: 2nd European geothermal workshop, France. 2013.

Gelet R, Loret B, Khalili N. A thermo–hydro–mechanical coupled model in local thermal non-equilibrium for fractured HDR reservoir with double porosity. J Geophys Res. 2012;B7:117.

Genter A, Castaing C, Dezayes C, Tenzer H, Traineau H, Villemin T. Comparative analysis of direct (core) and indirect (borehole imaging tools) collection of fracture data in the Hot Dry Rock Soultz reservoir (France), Journal of Geophysical Research, vol. 102, B7, 15419-15431. 1997.

Genter A, Cuenot N, Graff JJ, Schmittbuhl J, Villadangos G. La géothermie profonde en France : quelles leçons tirer du projet pilote de Soultz-sous-Forêts pour la réalisation d'un projet industriel à Rittershoffen. Revue Géologues. 2015 ; 185:97-101.

Gentier, S, Rachez, X, Dezayes, C, Blaisonneau, A, Genter, A., 2005. How to understand the effect of the hydraulic stimulation in terms of hydro-mechanical behaviour at Soultz-sous-Forêts (France). GRC Trans. 29, 159–166.

GeORG Potentiel géologique profond du Fossé Rhénan supérieur. Parties 1 à 4. 2013. http://www.geopo tenziale.eu.

Gérard A, Genter A, Kohl T, Lutz P, Rose P, Rummel F. The deep EGS (enhanced geothermal system) project at Soultz-sous-Forêts (Alsace, France). Geothermics. 2006;35(4):473–83.

Guillou-Frottier, L., Carre, C., Bourgine, B., Bouchot, V., Genter, A. Structure of hydrothermal convection in the Upper Rhine Graben as inferred from corrected temperature data and basin scale numerical models. Journal of Volcanology and Geothermal Research. 2013; 256:29-49.

Haas, IO, Hoffmann, CR. Temperature gradient in pechelbronn oil-bearing region, Lower Alsace: its determination and relation to oil reserves. AAPG Bulletin 1929;13(10):1257–1273.

Haenel R. Plateau Uplift. Geothermal investigations in the Rhenish Massif. Berlin: Springer; 1983. p. 228–46.

Huenges, E., Ledru, P.. Geothermal energy systems: exploration, development, and utilization. John Wiley & Sons, 2011.

Jain C, Vogt C, Clauser C. Maximum potential for geothermal power in germany based on engineered geothermal systems. Geothermal Energy. 2015;3(1):15.

Jaupart, C., Mareschal, J.C.. Heat generation and transport in the Earth. Cambridge university press, 2010.

Kestin J, Khalifa H.E, Correia R.J. Tables of the dynamic and kinematic viscosity of aqueous NaCl solutions in the temperature range 20-150°C and the pressure range 0.1-35 MPa. J Phys Chem Ref Data. 1981;10(1):71–88.

Kirk SS, Williamson DM. Structure and thermal properties of porous geological materials. AIP Conference Proc. 2012;1426:867–70.

Kohl T, Mègel T. Predictive modeling of reservoir response to hydraulic stimulations at the European EGS site Soultz-sous-Forêts. Int J Rock Mech Mining Sci. 2007;44(8):1118–31.

Kohl T, Bächler D, Rybach L. Steps towards a comprehensive thermo-hydraulic analysis of the HDR test site Soultz-sous-Forêts In: Proceedings world geothermal congress. 2000. p. 2671–6.

Kolditz O, Clauser C. Numerical simulation of flow and heat transfer in fractured crystalline rocks: application to the hot dry rock site in Rosemanowes (UK). Geothermics. 1998;27(1):1–23.

Lengliné O, Boubacar M, Schmittbuhl J. Seismicity related to the hydraulic stimulation of GRT-1, Rittershoffen, France.Geophys. JInt. 2017; 208 (1) :1704–15.

Lu, S.M.. A global review of enhanced geothermal system (EGS). Renewable and Sustainable Energy Reviews 2017.

Magnenet V, Fond C, Genter A, Schmittbuhl J. Two-dimensional THM modelling of the large scale natural hydrothermal circulation at Soultz-sous-Forêts. Geotherm Energy. 2014;2(1):17.

Maurer V, Cuenot N, Gaucher E, Grunberg M, Vergne J, Wodling H, Lehujeur M, Schmittbuhl J. Seismic monitoring of the Rittershoffen EGS project (Alsace, France) In: Proceedings world geothermal congress. 2015.

Pribnow D, Schellschmidt R. Thermal tracking of upper crustal fluid flow in the Rhine Graben. Geophys Res Lett. 2000;27(13):1957–60.

Pribnow D, Fesche W, Hägedorn F. Heat production and temperature to 5 km depth in HDR site in Soultz-sous-Forêts. GGA: Technical report; 1999.

Pruess K. Modeling of geothermal reservoirs: fundamental processes, computer simulation and field applications. Geothermics.

1990;19(1):3–15.

Rowe AM, Chou JCS. Pressure–volume–temperature-concentration relation of aqueous sodium chloride solutions. J Chem Eng Data. 1970;15(1):61–6.

Rummel F. Physical properties of the rock in the granitic section of borehole GPK1 Soultz-sous-Forêts. Geothermal energy in Europe: the Soultz Hot Dry Rock Project. 1992. p. 199–216.

Sanjuan B, Scheiber J, Gal F, Touzelet S, Genter A, Villadangos G. Inter-well chemical tracer testing at the Rittershoffen geothermal site (Alsace, France). In: European Geothermal Congress. 2016.

Sanjuan, B., Pinault, 674 J., Rose, P., Gerard, A., Brach, M., Braibant, G., Crouzet, C., Foucher, J., Gautier, A., Touzelet, S.. Geochemical fluid characteristics and main achievements about tracer tests at Soultz-sous-Forêts (France). In: EHDRA Scientific Conference. 2006. p. 1–13.

Sanyal SK, Butler SJ, Swenson D, Hardeman B. Review of the state-of-the-art of numerical simulation of enhanced geothermal systems. Trans. Geotherm. Resourc. Council. 2000; 28:181–6.

Sausse, J., Dezayes, C., Dorbath, L., Genter, A., Place, J. 3d model of fracture zones at Soultz-sous- Forêts based on geological data, image logs, induced microseismicity and vertical seismic profiles. Comptes Rendus Geoscience 2010;342(7):531–545.

Schaming, M., Grunberg, M., Jahn, M., Schmittbuhl, J., Cuenot, N., Genter, A., Dalmais, E. CDGP, the data center for deep geothermal data from alsace. In: EGU General Assembly Conference Abstracts. 18; 2016. p. 9897.

Schill, E., Genter, A., Cuenot, N., Kohl, T..Hydraulic performance history at the Soultz EGS reservoirs from stimulation and long-term circulation tests. Geothermics 2017;70:110–124.

Schindler, M., Baumgärtner, J., Gandy, T., Hauffe, P., Hettkamp, T., Menzel, H., Penzkofer, P., Teza, D., Tischner, T., Wahl, G.. Successful hydraulic stimulation techniques for electric power production in the Upper Rhine Graben, Central Europe. In: Proceedings World geothermal congress, 2010.

Tester, J., Anderson, B., Batchelor, A., Blackwell, D., Dipippo, R., Drake, E., Garnish, J., Livesay, B., Moore, C., Nichols, K., Toksöz M.N, ., Veatch, J.. The future of geothermal energy, Impact of Enhanced Geothermal Systems on the United States in the 21st century. Technical Report; MIT report; 2006.

Tomac, I., Sauter, M. A review on challenges in the assessment of geomechanical rock performance for deep geothermal reservoir development. Renewable and Sustainable Energy Reviews 2017.

Traineau, H., Genter, A., Cautru, J.P., Fabriol, H., Chevremont, P. Petrography of the granite massif from drill cutting analysis and well log interpretation in the geothermal HDR borehole GPK-1 (Soultz, Alsace, France). Geothermal Science and Technology 1991;3(1):1–29.

Valley B. The relation between natural fracturing and stress heterogeneities in deep-seated crystalline rocks at Soultz-sous-Foréts (France). PhD thesis, ETH Zürich. 2007.

Vallier B., Magnenet V., Schmittbuhl J., Fond C., THM modeling of hydrothermal circulation at Rittershoffen geothermal site, France. Geothermal Energy. 6:22. (2018).

Vallier B., Magnenet V., Schmittbuhl J., Fond C., Large scale hydro-thermal circulation in the deep geothermal reservoir of Soultz-sous-Forêts (France). Geothermics. 1:78. (2019).

Vidal J, Genter A, Schmittbuhl J. Pre- and post- stimulation characterization of geothermal well GRT-1, Rittershoffen, France: insights from acoustic image logs of hard fractured rocks. Geophys J Int. 2016a;206(2):845–60.

Vidal J, Patrier P. Genter A, Beaufort D. Occurrences of clay minerals in permeable fracture zones in the granitic basement of geothermal wells at Rittershoffen, France In: 42nd Workshop on geothermal engineering Stanford University, Stanford, California, February 13–15. 2017.

Watanabe K, Takahashi H. Fractal geometry characterization of geothermal reservoir fracture networks. J Geophys Res.1995;100:521–8.

Willis-Richards J, Watanabe K, Takahashi H. Progress toward a stochastic rock mechanics model of engineered geothermal systems. J Geophys Res. 1996; 101:17481–96.

Zaytsev ID, Aseyev GG. Properties of aqueous solutions of electrolytes. Boca Raton: CRC Press; 1992.